Available online at www.sciencedirect.com

SciVerse ScienceDirect

Procedia IUTAM 3 (2012) 67 – 75

Procedia IUTAM

www.elsevier.com/locate/procedia

Linking Scales in Computations: from Microstructure to Macro-scale Properties

Multi-scale modelling of the development of heterogeneous distributions of stress, strain, deformation texture and anisotropy in sheet metal forming

P. Van Houtte [a,*], J. Gawad[b,c], P. Eyckens[a], B. Van Bael[a,d], Giovanni Samaey[b], D. Roose[b]

[a]*Department MTM, Katholieke Universiteit Leuven,BE-3000 Leuven, Belgium*
[b]*Department Computer Science, Katholieke Universiteit Leuven,3000 Leuven, Belgium*
[c]*University of Science and Technology AGH, 30-049 Krakow, Poland*
[d]*Department IWT, Limburg Catholic University College, 3590 Diepenbeek, Belgium*

Elsevier use only: Received date here; revised date here; accepted date here

Abstract

A Finite Element (FE) method is used to simulate cup drawing of two sheet materials: a carbon steel (DC06) and an aluminium alloy (AA3103-O). The evolution of the deformation texture is simulated by the Taylor and ALAMEL models, and this in every integration point of the FE mesh. Such point is in fact treated as a representative volume element (RVE) at macro-scale, and consists of 5000 crystallites each with their own crystal orientation. Each time the texture is updated, the constitutive law which describes the anisotropic plastic response of the material at macro-scale is updated as well. The calculation time required for this is kept within reasonable limits thanks to an adaptive updating scheme. Comparisons of the predicted textures with textures measured at different locations have been done. The predicted and measured cup profiles have been compared as well. This made it possible to evaluate the increase in accuracy by taking texture updating into account or not.

Cup drawing; hierarchical multi-scale modelling; finite element method; plastic anisotropy; deformation texture; experimental validation

1. Introduction

In cup drawing or other sheet metal forming processes, the crystallographic texture in the material evolves. This evolution depends on the local deformation history. As this is usually different in every location of the sheet, the evolution of the texture will be heterogeneous as well. However, at any given time and location in the sheet, the constitutive law which describes the plastic response of the material at macro-scale, depends on the texture and should be known to the finite element (FE) model used to simulate the metal forming process. The present authors

* Corresponding author. Tel.: +32 16 321304; fax: +32 16 321990.
E-mail address: paul.vanhoutte@mtm.kuleuven.be.

 doi:10.1016/j.piutam.2012.03.005

prefer to use a rather conventional explicit elastic-plastic FE code in which the material response is described by a user-written routine (VUMAT). The element size is much larger than the grain size of the material. This means that integration points actually represent RVEs at macro-scale. The present authors assign a multi-crystal consisting to 5000 crystallites to each integration point. This relatively large number guarantees a sufficient accuracy when calculating the plastic anisotropy from the texture. For this latter operation, a method is used which leads to an analytical model for the anisotropic response of the material. Such approach is called "hierarchical multi-scale model". Other approaches will be shortly reviewed as well. A section will give more details about the several components of the VUMAT which has been implemented. The code optimisation needed to reduce the calculation effort will be explained. Finally the results of simulations of cup drawing of aluminium and steel sheets will be discussed, including the comparison of predicted cup profiles and deformation textures with measured ones.

2. Multi-scale modelling

The obvious approach to implement texture-based anisotropy into FE simulations of a forming process, would consist in representing the state variable "texture" as a discrete set of crystal orientations in each integration point, and use a polycrystal model (such as the well known Taylor model [1-2]) for two tasks: producing the stress-strain relationship each time it is needed, and simulate the texture evolution for each strain increment. This method will be called here the "embedded approach". Dawson et al. [3] have given a nice overview on the possibilities of this approach. Notice that it accounts automatically for texture evolution. However, it requires a quite large computational effort when applied to industrial problems. Also, not all models which can be used for the simulation of texture evolution are sufficiently reliable from a quantitative point of view (see below). This means that the predicted orientation distribution functions (ODF) are often not close enough to those that would be measured in validation experiments [4]. In addition, it is not only necessary to work with good models for deformation texture prediction. In order to make good predictions of plastic anisotropy such as *r*-values, it is also necessary to represent textures by a sufficiently large number of discrete crystal orientations. It is in this respect interesting to look at a case study in which an ODF had been transformed into 354 discrete crystal orientations. The *r*-values calculated from this discrete texture turned out to have errors up to 20 % when compared to *r*-values directly calculated from the ODF using methods based on spherical harmonics (figure 3 in [5]). This error was reduced to 0.5 % when the number of orientations in the discrete set was increased to 1970. Note in addition that the texture used in this case study had an orthorombic sample symmetry, which strongly reduces the required size of the discrete set [4]. In the context of the present paper, the presence of such sample symmetry cannot be taken for granted; therefore, discrete sets with no less than 5000 grain orientations have been used. It is furthermore necessary to work with polycrystal models which makes quantitatively reliable predictions of deformation textures. The well-known Taylor model [1] does not perform well in this regard (see Table 3 and Fig. 7 in [2]). The crystal plasticity finite element model (CPFEM) (see e.g. [6]) would perform much better. Unfortunately, it would lead to unaffordable calculation times in the present context. The crystal-plasticity fast Fourier method (CPFFT) might remedy this [7] in the future. Anyway, much faster than CPFEM models are the so-called Taylor-type models. Some of these, namely the "grain interaction" models (GIA [8] and the ALAMEL [2]) have been proved to represent a good compromise between the Taylor model and CPFEM (see Table 3 and Fig. 7 in [2] and Fig. 5 in [9]). In these models, stress equilibrium at grain boundaries is taken into account to a certain extent, hereby sacrificing the perfect homogeneity of plastic strain which is assumed by the Taylor model. Three length scales would be linked by an 'embedded multi-scale model' consisting of a FE method which uses either a Taylor, GIA or ALAMEL model as constitutive model. Recently Roters et al. [10] have however advocated the use of a hierarchical multi-scale model, because the embedded method is too calculation intensive. Finally the present authors have decided to develop a hierarchical approach which will be presented here. It uses virtual mechanical tests in order to identify an anisotropic constitutive law in the form of an analytical expression of which the coefficients need to be determined. Each time the constitutive model needs to be obtained from the freshly updated texture, a polycrystal model (Taylor or ALAMEL) performs a series of virtual mechanical tests, taking the texture into account. The constitutive law identified in this way (Facet method [11]) can treat all possible strain or stress modes within a given angular resolution in stress/ strain rate space. This could be done once and for all in the beginning of the FE simulation thus producing an anisotropic constitutive model to be used in all integration points and all strain increments. This would lead to a rather fast hierarchical multi-scale model which would however not simulate texture evolution, as the embedded approach would do.

Instead, it is of course possible to update the texture after each strain increment using a polycrystal model, after which the constitutive law can also be updated by means of virtual experiments. Such hierarchical approach would however be most calculation intensive. This is the reason why a code optimization strategy, which achieves a dramatic speed-up of the calculation procedure, will be presented here.

3. Short Description of the Model

3.1. Constitutive Model

The commercial FE software program Abaqus/Explicit was used. A user material routine (VUMAT) has been developed which has to perform the following tasks. A 'state variable' consisting of 5000 crystal orientations and associated weight factors (i.e. a discrete texture) must be introduced in each integration point. Texture updates and updates of the constitutive law must be organized, not after each strain increment, but only when a specific command is issued to that purpose (see below). In that case, one of the polycrystal models (Taylor or ALAMEL [2]) is invoked. After the texture update, the constitutive material law of the integration point, based on the Facet method [11], must also be updated. This method is now briefly reminded. Plastic incompressibility and rate-insensitivity are assumed. A stress differential effect can be implemented when needed. The plastic work per unit volume is expressed by the following homogeneous polynomial of degree n in function of the plastic strain rate $\mathbf{D}$:

$$\psi(\mathbf{D}) = \left[\sum_{\kappa=1}^{K} \lambda_\kappa (\mathbf{S}_\kappa : \mathbf{D})^n \right]^{\frac{1}{n}} \tag{1}$$

where n is an even integer larger than 1; in the present work, the value 6 was used. The parameters $\mathbf{S}_\kappa$ are obtained from the polycrystal model at the time that it performs the virtual mechanical tests. Each test is described by a pre-defined plastic strain mode. There are K of them; they are nearly equidistant in strain rate space. In the present work, K=201. For each of these, the polycrystal code calculates the stress deviator $\mathbf{S}_\kappa$ which a material with the current texture would require in order to undergo the prescribed plastic strain. The parameters λ_κ are obtained by non-negative least squares fitting to the polycrystal plasticity results for a given texture. They must be non-negative because in that case, the constitutive law is strictly convex [11]. Finally the function $\psi(\mathbf{D})$ can be used as a plastic potential in strain rate space [12]: the derivative of $\psi(\mathbf{D})$ with respect to $\mathbf{D}$ then yields the stress deviator $\mathbf{S}$ which corresponds to a given plastic strain rate tensor $\mathbf{D}$:

$$\mathbf{S} = \frac{\partial \psi(\mathbf{D})}{\partial \mathbf{D}} \tag{2}$$

3.2. Polycrystal Model

Two polycrystal models have been used for the updating of the deformation textures and for running the virtual mechanical tests which are used to identify the Facet model: the Taylor model and the ALAMEL model [2]. These polycrystal models are two-scale models for single-phase metallic materials. Suppose that a deformation history is specified at the macro-scale by prescribing a series of deformation increments, each described by a displacement gradient. The nominal strain of each increment is typically of the order of 1 %. The versions of the polycrystal models used in the present work neglect the elastic part of the deformation. The Taylor model assumes that the meso-scale deformation (i.e. the plastic deformation of each grain in the discrete set) is equal to the prescribed macro-scale deformation. It is then assumed that in a given grain, the deformation is achieved by dislocation glide. The symmetric part of the displacement gradients are used to calculate the slips on each of the slip systems, hereby minimizing the total dissipated plastic work. For fcc metals, {111}<110> slip systems are adopted, and for bcc metals, {110}<111> + {112}<111> systems. This is equivalent with using the generalized Schmid law [2]. Once

the slip rates have been found, the rotation of the crystal lattice can be calculated, taking the skew-symmetrical parts of the displacement gradient tensors into account. The rotated crystal orientations effectively define the updated texture. In this process, the stress deviators in the crystals are obtained as well. Their volume average is used as the macroscopic stress deviator felt at the macro-scale. This is why these models can also be used to perform the virtual mechanical tests. Note that, when necessary, it is possible to implement almost any work hardening model (defined at grain scale) in such polycrystal model. The results of the present study (deformation textures, cup profiles) were very insensitive to the particular choice of the work hardening model; neither would they be sensitive to the choice of a model for strain rate sensitivity, if that were used. This means that the method proposed in the present paper would also work with visco-plastic versions of the Taylor or ALAMEL models, probably leading to similar results.

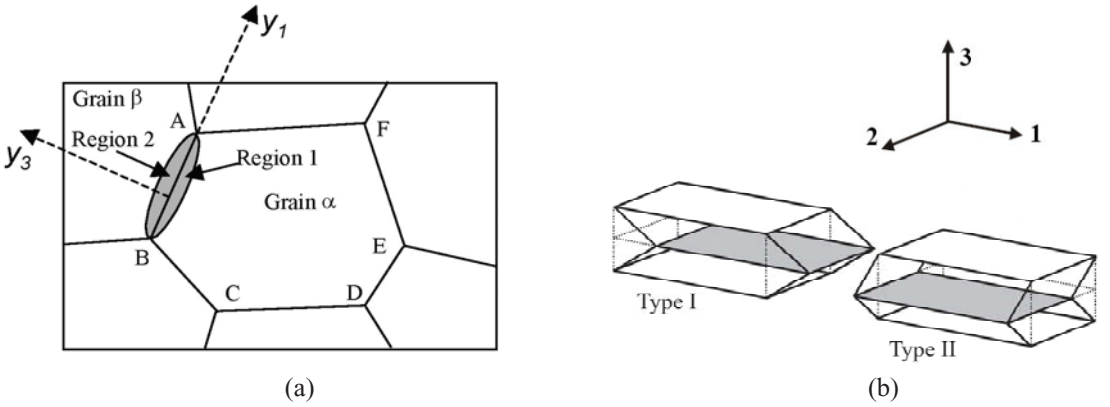

Fig. 1. After [2]. (a) Schematic representation of a microstructure as assumed by the ALAMEL model. (b) Type I or Type II: grain cluster which is supposed to be located at a grain boundary segment. Bottom, top grain = region 1, 2 in (a); axis 3 = axis y_3 in (a). Type I and II illustrate strain relaxations which are possible.

The Advanced Lamel (ALAMEL) Model is a variant of the Taylor model. It does not assume that the stress and strain fields inside a given crystal are homogeneous, as is done by the Taylor model. However, it does not try to calculate the complete field of velocity gradients, slip rates and stresses inside the grain. Instead, it will only estimate these in very shallow regions close to the grain boundaries. Region 1 (Fig. 1a) is such region in grain α. Note that the solution for region 1 is not obtained independently of what happens in the neighbouring grain β. The model will indeed simultaneously solve for the slip rates in regions 1 and 2, thereby taking the stress equilibrium along common the grain boundary into account. The method used is the following: (i) the average strain rates of region 1 and region 2 taken together should be equal to the prescribed macroscopic strain; (ii) this leaves two free parameters (degrees of freedom) which do not exist in the Taylor model, in the form of free simple shear relaxations in each of the two regions. Fig. 1b shows the configuration of these free simple shear relaxations. There are two types: Type I and Type II. It is seen that for each type, the "free simple shear" in region 1 is exactly opposite to that in region 2. It has been proven that this is one way of guaranteeing the equilibrium of the two shear stresses which act on the common grain boundary [2]. It is seen that the slip rates are not estimated in the centre of a grain, as the FC Taylor model would implicitly do, but rather at grain boundaries (Fig. 1a). It is then for those locations (region 1 and region 2) that the texture evolution is calculated. Their initial crystal orientations are chosen at random from the ODF of the initial material. So far, the initial orientation of the grain boundary is chosen at random. The evolution of this orientation with deformation is also simulated by the model. Region 1, region 2 and their common grain boundary taken together are called a 'cluster'. In the present work, the ALAMEL model made use of 2500 clusters, which means a total of 5000 grain orientations. The discrete crystallographic texture (initial, or after deformation) consisting of the grain orientations of these 5000 grains is believed to be representative for the overall deformation texture of the polycrystal, in spite of the fact that no crystal orientations of locations in the centres of the grains have been considered. This assumption has been validated in several studies [2,9]; however, theoretical proof is lacking.

3.3. Code optimization

A cluster computer consisting of 256 Opteron dual-core processors was used to run the model. The Abaqus Explicit FE software was always run on a single node. However, extra nodes were used for updating the texture and for the identification of the Facet model. Each time such update was necessary in a given integration point, it was checked whether some other node of the machine happened to be idle. If so, a request for an extra node for a relatively short time was issued, as such update needs only about 10 min on a node. In a particular test run, 5939 updates needed to be done, which would have required 43 days of calculation on a single node; however, by distributing the update tasks over other nodes, this was reduced to 1.57 days. A further optimization has been made possible by adaptive scheduling of the updates. In a given integration point, updates were not requested after every strain increment, but only when certain requirements were met. The main requirement was, that the total strain P_{cr} which the material of the integration point had undergone since the last update, should not be smaller than some prescribed lower limit. A value of about 3 % was used in the present work. The motivation of this was, that the deformation texture and the shape of the yield locus do not change very rapidly with ongoing strain. In one of the simulations of a cup drawing process with ~3000 integration points, there were 11 x 10^6 crystallites in all discrete textures together. Using a value 0.03062 for P_{cr} (combined with an additional updating requirement that the FE step number must be a multiple of 300), 33445 updates turned out to be needed. The total wall-clock calculation time was approximately 5 days on the cluster computer. About 230 days would have been needed on a single node.

4. Experimental and simulated cup drawing tests

4.1. Experimental Results

Table 1. Description of materials and cup drawing tests. Punch and die: (50R7 means: diameter 50mm, fillet radius 7mm). Blank holder force: BHF. Friction coefficient used during the simulation: μ.

Grade	Thickness [mm]	Composition [mass %]	Blank [mm]	Punch	Die	BHF [kN]	μ
DC06	0.70	0.02%C, 0.25%Mn, 0.30%Ti	100	50R7	52R6	10	0.10
AA3103-O	0.85	0.2%Si, 1.0%Mn, 0.7%Fe	100	50R5	52.5R10	5	0.05

It was decided to use cup drawing tests for the first validation of the method. After drawing of a perfectly circular blank, the variations of the height of the cup wall may vary because of the anisotropy of the material. This is called "earing" and it is undesired in industry. These variations depend on the crystallographic texture. It has been, and still is, a challenge for metal forming software to correctly predict this earing profile. Depending on the texture, the earing tendency may be strong, and that case, it can easily be qualitatively predicted by software which uses an anisotropic constitutive model which has been identified before the simulation, either using the results of mechanical tests or by implementing information derived from a measurement of the texture of the material. However, modern materials for the production of cans have a much reduced earing tendency - which the industry ever wants to reduce further. Good predictions of the remaining earing tendency then become difficult, and will require taking texture evolution into account. This has been a motivation to compare results obtained with texture evolution to those obtained without texture evolution, as will be given below. Experimental results for two materials have been compared with simulation results. The two materials were: DC06 (an interstitial-free steel) and AA3103-O (an Al-Si-Mn-Fe alloy). The materials had been cold rolled and annealed before testing. DC06 had also been skin-passed after annealing. Table 1 summarizes the characteristics of materials and cup drawing tests, as well the blank holder forces and the friction coefficients used in the simulations. Fig. 2 shows the resulting earing profiles.

4.2. Simulation Results

The symmetry of the blanks, which initially had a circular shape, made it possible to limit the calculation to one

quarter. It was modelled by three layers of brick elements with reduced integration (C3D8R), 3096 elements in total. The texture in each integration point was described by 5000 discrete orientations. Simulations I and II used the ALAMEL polycrystal deformation model while III used the Taylor model. Texture updating was done in simulation II. Table 1 gives the values of the friction coefficients used during the simulation.

5. Comparison of experimental and simulated results

5.1. Earing profiles

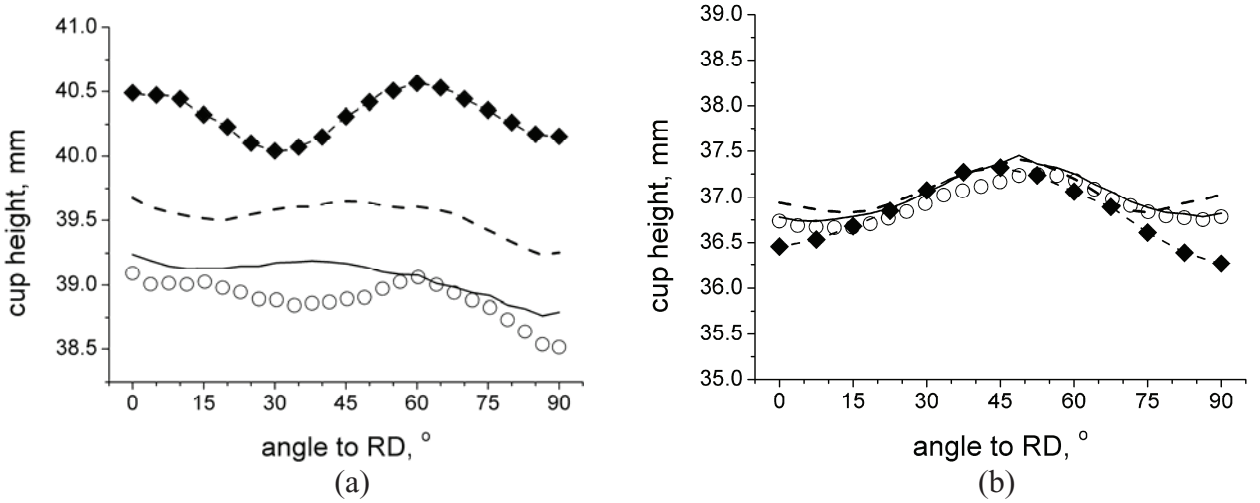

Fig. 2 After [13]. (a) DC06, (b) AA3103-O. *Dashes with filled symbols*: experimental cup profiles. The die geometry of the simulations corresponds with the tools used for the experiments. *Full line*: simulation I. *Circles*: simulation II. *Dashes*: simulation III.

Fig. 2 shows both experimental and simulated results for the earing profiles (cup wall height). The wall height of the experimentally drawn cups (DC06 material) feature local maxima at 0° and 60° (Fig. 2a). In a full 360° range, the maximum at 0° leads to 2 ears and the one at 60° to 4 ears, amounting to 6 ears in total. The simulations were based on the tool geometry of the experimental setup. Simulations I and III, in which texture was not updated, both lead to a flatter shape with valleys at 90° (i.e. TD). When texture evolution is taken into account (simulation II, using ALAMEL), a 6-ear developing behaviour appears, with ears at RD and at 60°. This result compares well with the experimental findings, except that the global cup height is underestimated by about 1.5 mm. This could be due to an inappropriate choice of the friction coefficient, of which the value had been arbitrarily fixed to 0.1; other values have not been tried out. As for the AA3103-O material, all simulated curves nearly coincide, reproducing the experimental maximum at 45° (Fig. 2b).

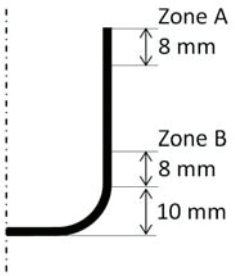

Fig. 3 After [13]. Locations of the samples taken for texture measurements in the cup wall. A = near the rim: zone; B = near the bottom.

5.2. Textures

Samples for texture measurements have been taken from the drawn cups at half sheet thickness at 0°, 45° and 90° with respect to the rolling direction. Fig. 3 shows where they were taken. Fig. 4 shows examples of measured and simulated textures for both materials. The textures are represented by means of φ_2=45° sections of the ODF [4]. Note that the symmetry options for such ODF need to be: cubic/triclinic. "Triclinic" means that sample symmetry (statistical type of symmetry, see [4]. This is NOT a symmetry of the geometry of the cup drawing process!) cannot be taken into account, because it is not known in advance whether or not the initial sample symmetry of the material will be maintained during the deformation process. Indeed, the FE code may come up with velocity gradient tensors which may feature shears of all sorts, which would destroy the initial sample symmetry of the texture, when present. So the texture data sets on which the polycrystal models (Taylor or ALAMEL in the present case) operate cannot be reduced in size by taking advantage of sample symmetry.

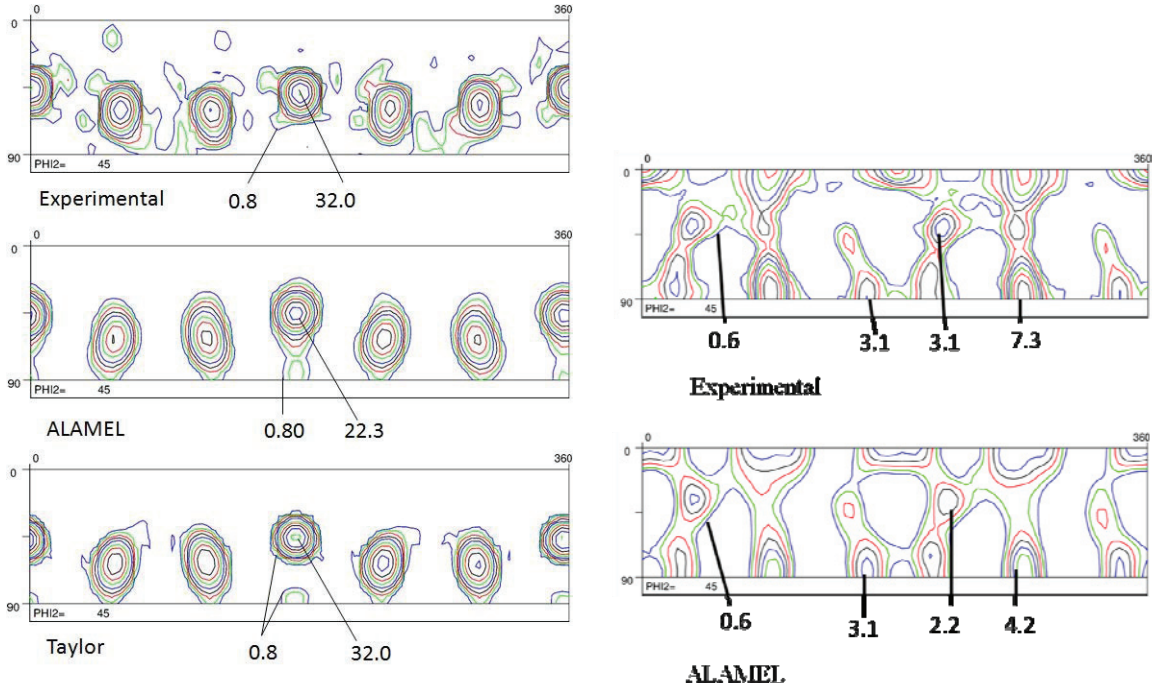

(a) (b)

Fig. 4 (a) After [13]. φ_2=45° sections of the ODF of measured and simulated textures for DC06 at location A, 90° from RD (see fig. 3). Texture evolution simulated with ALAMEL and Taylor. (b) φ_2=45° sections of the ODF of measured and simulated textures for AA3103-O at location A, 45° from RD. Texture evolution simulated with ALAMEL.

ODFs are probability distribution functions defined in orientation space, which is a curved 3-d space [4]. To assess the difference between the measured texture and the predicted one, an error measure is used which only vanishes when the experimental ODF $f_{\mathrm{ref}}(g)$ and the predicted ODF $f_{\mathrm{sim}}(g)$ are equal in all points of orientation space. It is defined as the integral over entire orientation space of the squared difference of $f_{\mathrm{sim}}(g)$ and $f_{\mathrm{ref}}(g)$, divided by the integral of the square of the experimental texture (i.e. its texture index TI):

$$\frac{\Delta \mathrm{ODF}}{\mathrm{T.I.}} = \frac{\int \left(f_{\mathrm{sim}} - f_{\mathrm{ref}}\right)^2 dg}{\int f_{\mathrm{ref}}^2(g) dg} = \frac{\int \left(f_{\mathrm{sim}} - f_{\mathrm{ref}}\right)^2 dg}{TI_{\mathrm{ref}}} \,. \tag{3}$$

This measure will be called "normalized ODF difference". The values obtained for DC06 and AA3103-O along 3 directions with respect to the rolling direction in zones A and B are given in Table 2. It is seen that for DC06, at location A and at 45° from the rolling direction, ΔODF/T.I. is around 0.09 for ALAMEL and 0.16 for Taylor. Fig. 4a allows to visually inspect these two textures in order to compare them. The rather high value of ΔODF/T.I. for Taylor is mostly due to the fact that in general, the textures predicted by the Taylor model are too sharp. It must be admitted that this extremely low value of 0.09 is not always achieved by ALAMEL. However, it is clear from Table 2 that the ALAMEL model systematically provides more accurate predictions than the Taylor model.

Table 2. Normalized ODF difference between the final updated textures and the final experimental texture for DC06 and AA3103-O along 3 directions with respect to the rolling direction in zones A and B. Texture evolution: calculated using the ALAMEL or the Taylor model.

Material	Model	ΔODF/T.I. for Zone:	0°	45°	90°
DC06	Taylor	A	0.37	0.16	0.23
		B	0.19	0.24	0.31
	ALAMEL	A	0.16	0.09	0.23
		B	0.16	0.16	0.26
AA3103–O	ALAMEL	A	0.25	0.15	0.16
		B	0.16	0.18	0.15

6. Conclusions

It has been demonstrated that full-field texture predictions by fully coupled FE simulations of sheet metal forming operations are feasible. The required computer system does not need to be exceptionally powerful and would be within reach of most research institutions. This was made possible by optimizing the code in various ways. A cup drawing simulation with ~2000 integration points, each with a discrete texture consisting of 5000 grains, could be carried out in 5 days on a quite common cluster computer which was shared with other users. In addition, the heterogeneous field of deformation textures which was obtained during these simulations for DC06 and AA3103-O sheets corresponded rather well with experimentally measured textures. A quantitative criterion was used for this comparison. This also demonstrates the accuracy of the multi-scale model in which the ALAMEL model for polycrystal plasticity is the cornerstone. The ALAMEL model certainly performed better than the Taylor model in all cases. Similar comparisons between ALAMEL and Taylor are planned for other materials. There is an indication that subtle details of the deformation pattern in metal forming, such as 6-ear earing profiles, can only be predicted by a fully coupled multi-scale models which take texture evolution into account.

Acknowledgements

The authors gratefully acknowledge the financial support from the project IDO/08/09, funded by K.U.Leuven, and from the Belgian Federal Science Policy agency, contracts IAP6/24 and IAP6/4. They also thank the companies TataSteel, ArcelorMittal and Aleris for the sheet materials and cup drawing experiments. GS is Postdoctoral Fellow of the Research Foundation – Flanders (FWO).

References

[1] Taylor GI. Plastic strain in metals. *J. Inst. Metals* 1938; **62**: 307-324.

[2] Van Houtte P, Li S, Seefeldt M, Delannay L. Deformation texture prediction: from the Taylor model to the advanced Lamel model. *Int. J. Plasticity* 2005; **21**: 589-624.

[3] Dawson PR, MacEwen SR, Wu PD. Advances in sheet metal forming analyses: dealing with mechanical anisotropy from crystallographic texture. *International Materials Reviews* 2003; **48**: 86-122.

[4] Bunge HJ. *Texture analysis in material science*. London: Butterworths; 1982.

[5] Toth LS, Van Houtte P. Discretization techniques for orientation distribution functions. *Textures and Microstructures* 1992; **19**: 229-244.

[6] Kalidindi SR, Bronkhorst CA, Anand L. Crystallographic texture evolution in bulk deformation processing of FCC Metal., *J. Mech. Phys. Solids* 1992; **40**: 537-569.

[7] Liu B, Raabe D, Roters F, Eisenlohr P, Lebensohn RA. Comparison of finite element and fast Fourier transform crystal plasticity solvers for texture prediction, *Modelling Simul. Mater. Sci. Eng*. 2010; **18**: 085005.

[8] Crumbach M, Pomana G, Wagner P, Gottstein G. A Taylor type deformation texture model considering grain interaction and material properties. Part I - Fundamentals. In: Gottstein G, Molodov DA, editors. *Recrystallisation and Grain Growth (Proc. First Joint Conference)*, Berlin: Springer; 2001, p. 1053-1060.

[9] Van Houtte P, Li S, Engler O. Modelling deformation texture of aluminium alloys using grain interaction models. *Aluminium* 2004; **80/6**: 702-706.

[10] Roters F, Eisenlohr P, Hantcherli L, Tjahjanto DD, Bieler TR, Raabe D. Overview of constitutive laws, kinematics, homogenization and multiscale methods in crystal plasticity finite-element modeling: Theory, experiments, applications. *Acta Mater.* 2010; **58**: 1152-1211.

[11] Van Houtte P, Yerra SK, Van Bael A. The Facet method: A hierarchical multilevel modelling scheme for anisotropic convex plastic potentials. Int. J. Plasticity 2009; **25**: 332-360.

[12] Van Houtte P. Application of plastic potentials to strain rate sensitive and insensitive anisotropic materials. *Int. J. Plasticity* 1994; **10**: 719-748.

[13] Van Houtte P, Gawad J, Eyckens P, Van Bael B, Samaey G, Roose D. An efficient strategy to take texture-induced anisotropy point-by-point into account during FE simulations of metal forming processes, submitted to: *Proc. International Conference on Textures of Materials 16 (ICOTOM 16)*, IIT Mumbai (2011).